A Hyper Suprime-Cam View of the Interacting Galaxies of the M81 Group

Citation for published version:
Okamoto, S, Arimoto, N, Ferguson, AMN, Bernard, EJ, Irwin, MJ, Yamada, Y & Utsumi, Y 2015, 'A Hyper Suprime-Cam View of the Interacting Galaxies of the M81 Group' Astrophysical Journal Letters, vol. 809, no. 1. DOI: 10.1088/2041-8205/809/1/L1

Digital Object Identifier (DOI):
10.1088/2041-8205/809/1/L1

Link:
Link to publication record in Edinburgh Research Explorer

Document Version:
Publisher's PDF, also known as Version of record

Published In:
Astrophysical Journal Letters

The Astrophysical Journal Letters, 809:L1 (6pp), 2015 August 10 doi:10.1088/2041-8205/809/1/L1

A HYPER SUPRIME-CAM VIEW OF THE INTERACTING GALAXIES OF THE M81 GROUP*

Sakurako Okamoto[1], Nobuo Arimoto[2,3], Annette M. N. Ferguson[4], Edouard J. Bernard[4],
Mike J. Irwin[5], Yoshihiko Yamada[6], and Yousuke Utsumi[7]
[1] Shanghai Astronomical Observatory, 80 Nandan Road, Shanghai 200030, China; sakurako.okamoto@gmail.ac.jp
[2] Subaru Telescope, National Astronomical Observatory of Japan, 650 North A'ohoku Place, Hilo, HI 96720, USA
[3] The Graduate University for Advanced Studies, Osawa 2-21-1, Mitaka, Tokyo 181-8588, Japan
[4] Institute for Astronomy, University of Edinburgh, Royal Observatory, Blackford Hill, Edinburgh EH9 3HJ UK
[5] Institute of Astronomy, University of Cambridge, Madingley Road, Cambridge CB3 0HA, UK
[6] National Astronomical Observatory of Japan, Osawa 2-21-1, Mitaka, Tokyo 181-8588, Japan
[7] Hiroshima Astrophysical Science Center, Hiroshima University, Kagamiyama 1-3-1, Higashi-Hiroshima, Hiroshima 739-8526, Japan
Received 2015 June 19; accepted 2015 July 14; published 2015 August 4

ABSTRACT

We present the first results of a wide-field mapping survey of the M81 group conducted with Hyper Suprime-Cam on the *Subaru* Telescope. Our deep photometry reaches ∼2 mag below the tip of the red giant branch (RGB) and reveals the spatial distribution of both old and young stars over an area of ∼100 × 115 kpc at the distance of M81. The young stars (∼30–160 Myr old) closely follow the neutral hydrogen distribution and can be found in a stellar stream between M81 and NGC 3077 and in numerous outlying stellar associations, including the known concentrations of Arp's Loop, Holmberg IX, an arc in the halo of M82, BK3N, and the Garland. Many of these groupings do not have counterparts in the RGB maps, suggesting they may be genuinely young systems. Our survey also reveals for the first time the very extended ($\geqslant 2 \times R_{25}$) halos of RGB stars around M81, M82, and NGC 3077, as well as faint tidal streams that link these systems. The halos of M82 and NGC 3077 exhibit highly disturbed morphologies, presumably a consequence of the recent gravitational encounter and their ongoing disruption. While the halos of M81 and NGC 3077 and the inner halo of M82 have similar $(g-i)_0$ colors, the outer halo of M82 is significantly bluer indicating it is more metal poor. Remarkably, our deep panoramic view of the M81 group demonstrates that the complexity long known to be present in HI is equally matched in the low surface brightness stellar component.

Key words: galaxies: groups: individual (M81) – galaxies: individual (M81, M82, NGC 3077) – galaxies: interactions – galaxies: stellar content

1. INTRODUCTION

Over the last decade, deep studies of nearby galaxies have led to the discovery of vast stellar envelopes that are often rich in substructure (Mihos et al. 2005; Martínez-Delgado et al. 2010). These components are naturally predicted in models of hierarchical galaxy assembly, and their observed properties place important constraints on the amount, nature, and history of satellite accretion (e.g., Bullock & Johnston 2005; Pillepich et al. 2014). Due to their very low surface brightness, one of the most effective ways of mapping the peripheral regions of galaxies is through resolved star studies. For example, dedicated surveys of red giant branch (RGB) stars around M31 have revealed a stellar halo extending to more than ∼200 kpc that is dominated by tidal debris features (e.g., Ibata et al. 2001, 2014; Ferguson et al. 2002; McConnachie et al. 2009). Similarly, the Sloan Digital Sky Survey (SDSS) has been used to explore main-sequence (MS) turn-off stars in the halo of the Milky Way, leading to many discoveries of new substructures and satellites and a refined characterization of halo and thick-disk properties (e.g., Belokurov et al. 2007).

Using wide-field cameras equipped to 8 m class telescopes, it has recently become possible to extend these studies to systems beyond the Local Group (e.g., Mouhcine et al. 2010; Barker et al. 2012; Crnojević et al. 2013). Located at a distance of 3.6 Mpc (Freedman et al. 1994), M81 is a prime target for wide-field mapping of its resolved stellar content. Spectacular neutral hydrogen images have demonstrated the significant tidal interactions between M81 and its two brightest neighbors, M82 and NGC 3077, which modeling suggests have taken place in the last 300 Myr (e.g., van der Hulst 1979; Yun et al. 1994, 1999; Chynoweth et al. 2008). Deep photometry from the *Hubble Space Telescope* (*HST*) has been used to argue that the outlying HI concentrations of Arp's Loop (AL) and Holmberg IX (HoIX) may be tidal dwarf galaxies formed as a result of these interactions (Makarova et al. 2002; de Mello et al. 2008; Sabbi et al. 2008). In NGC 3077, 90% of the atomic hydrogen is located eastward of the center, in the tidal arm called "the Garland" where young stars have been observed (Karachentsev et al. 1985; Sakai & Madore 2001; Weisz et al. 2008). Several other young star concentrations have been associated with peaks in the HI gas (Durrell et al. 2004; Sun et al. 2005; Davidge 2008b; Mouhcine & Ibata 2009; Chiboucas et al. 2013); however, the global properties of this population throughout the M81 group are still poorly known.

The old stellar content around M81 has also been studied using large telescopes. Barker et al. (2009) found the evidence for a faint, extended structural component beyond the bright optical disk of M81 from wide-field images taken by *Subaru*/Suprime-Cam. They detected no color gradient in this structure out to 44 kpc; Monachesi et al. (2013) used *HST* pointings to extend this result to 50 kpc. Chiboucas et al. (2013) confirmed 12 new dwarf satellites as members of the M81 group, discovered from a 65 deg^2 survey with the Canada–France–Hawaii Telescope/MegaCam.

---

* Based on data collected at *Subaru* Telescope, which is operated by the National Astronomical Observatory of Japan.

In this Letter, we present the first results from a deep wide-field imaging survey of the M81 group that we are conducting with the new prime-focus imager, Hyper Suprime-Cam (HSC), on the *Subaru* Telescope. We report on the analysis of the inner 4 $\deg^2$ area, corresponding to a region spanning 100×115 kpc at the distance of the galaxy, which reveals the first truly panoramic view of the low surface brightness stellar component. The observations and data reduction are described in Section 2. Sections 3 and 4 present our analysis and results, which are discussed and concluded in Section 5.

For this Letter, we adopt a distance modulus for M81 and associated systems of $(m-M)_0 = 27.79$ (Radburn-Smith et al. 2011); position angles for M81, M82, and NGC 3077 of 157°, $67\overset{\circ}{.}5$, and $55\overset{\circ}{.}0$ east of north; and R_{25} radii for M81, M82, NGC 3077, and HoIX of $13\overset{\prime}{.}8$, $5\overset{\prime}{.}6$, $2\overset{\prime}{.}7$ and $2\overset{\prime}{.}5$, respectively (de Vaucouleurs et al. 1991; Karachentsev et al. 2004).

2. OBSERVATIONS AND DATA REDUCTION

We observed the central region of the M81 group in the g and i bands using four pointings of *Subaru*/HSC during the nights of 2015 January 21 and 22 (PI: S. Okamoto; Proposal ID: S14B-101) with the seeing ranged from $0\overset{\prime\prime}{.}6$ to $0\overset{\prime\prime}{.}9$. The HSC consists of 104 CCD detectors and provides a field of view of 1.76 $\deg^2$ with a pixel scale of $0\overset{\prime\prime}{.}17$ (Miyazaki et al. 2012). The observations were obtained as part of a survey to map the M81 group with seven HSC pointings. In this Letter, we focus on the inner 4 $\deg^2$ of our survey that overlaps the SDSS footprint (York et al. 2000).

The raw images were processed using the HSC pipeline (version 3.2.2), which is based on a software suite being developed for the Large Synoptic Survey Telescope (LSST) project (Ivezic et al. 2008; Axelrod et al. 2010). For the processed images, the DAOPHOT in IRAF was used to obtain the point-spread function photometry of resolved stars (Stetson 1987). Astrometric and photometric calibrations were done using the SDSS catalog. Artificial star tests were performed on some parts of the reduced images using the ADDSTAR in DAOPHOT, and indicate that our photometry is at least 50% complete to 26 mag in both bands, except for the inner regions of galaxies. We separate point sources from extended sources in the same manner as for Suprime-Cam images in Okamoto et al. (2012). Full details of the observations and data reduction will be presented in a forthcoming paper.

3. THE COLOR–MAGNITUDE DIAGRAMS

Figure 1 shows the resulting color–magnitude diagram (CMD) of roughly 550,000 point sources found in the whole 4 $\deg^2$ field. The error bars represent the photometric errors at $(g-i)_0 = 0$, as estimated by the artificial star tests. The Galactic extinction is taken from Schlafly & Finkbeiner (2011). Since the extinction varies across the observed field, we apply a reddening correction to each source individually according to its location, assuming a Fitzpatrick (1999) reddening law with $R_V = 3.1$. The central region within $r = 15'$ of M82 in the reddening map shows significantly higher extinction $E(B-V) \sim 0.16$ that includes the internal reddening of M82. Therefore, we replace it with $E(B-V) = 0.075$.

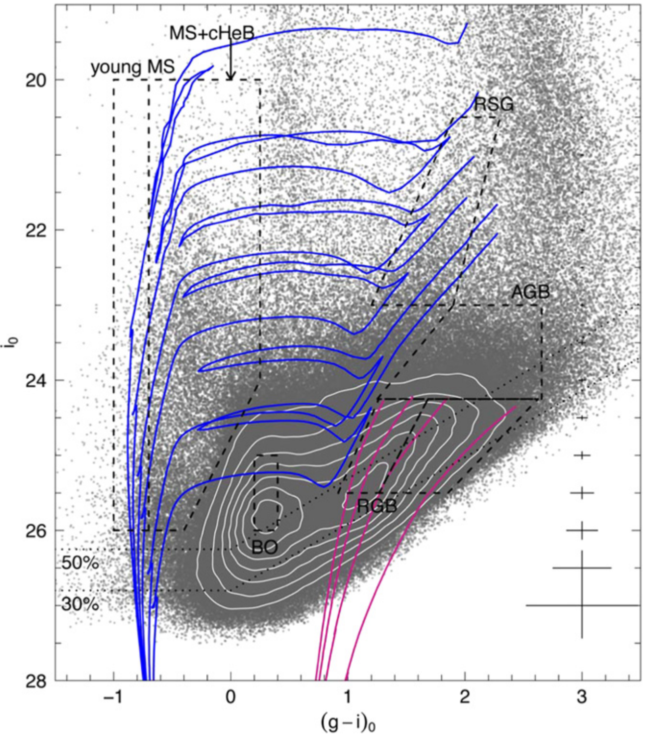

Figure 1. Dereddened CMD of stellar objects located within the central 4 $\deg^2$ area. The dashed boxes delineate the selection criteria for different stellar populations and are used to construct the maps presented in Figure 3. Theoretical Padova isochrones, adjusted at $(m-M)_0 = 27.79$, are shown for a 12 Gyr old population with $[M/H] = -2.2, -1.75, -1.3, -0.75$ from the left to the right (magenta) and for an $[M/H] = -0.75$ population with ages of 10, 18, 32, 50, 100, 160 Myr from top to bottom (blue). The dotted lines represent the completeness levels of 50% and 30%.

To aid in understanding the range of stellar populations present, theoretical Padova isochrones are overlaid (Bressan et al. 2012). We find that tracks with metallicity [M/H] varying from $\sim$0.0 to below -1.0 for young stars and $[M/H] \lesssim -1.0$ for old stars provide a good description of the data, in agreement with other studies of smaller regions (Makarova et al. 2002; Barker et al. 2009; Williams et al. 2009; Durrell et al. 2010; Kudritzki et al. 2012; Monachesi et al. 2013). We use $[M/H] = -0.75$ as the fiducial value for the young population and overlay the 10–160 Myr old isochrones as blue solid lines in Figure 1. For the old population, we plot $[M/H] = -2.2$ to -0.75 isochrones of 12 Gyr old as magenta solid lines.

Figure 1 is mostly populated by old RGB stars located at $i_0 \gtrsim 24$ and $(g-i)_0 \sim 1.2$. As discussed by Barker et al. (2009), the overdensity at $i_0 \sim 26$ and $(g-i)_0 \sim 0.3$ (labeled BO for "blue objects") mostly samples unresolved background sources. On the blue side of the foreground Galactic dwarf sequence (at $(g-i)_0 \sim 0.4$), young MS and core helium burning (cHeB) stars in the M81 group are found. We select stars in different evolutionary phases as shown by the dashed boxes in Figure 1: MS, cHeB, red supergiant (RSG), asymptotic giant branch (AGB), and RGB stars. The boundaries were adopted to limit the number of foreground/background contaminants. The young MS box mainly contains stars younger than $\sim$50 Myr old, while the MS+cHeB box is occupied by MS and post-MS stars of $<$100 Myr old. On the red bright side, the polygon contains RSGs about 25–160 Myr old with some contamination from Galactic disk stars. Above

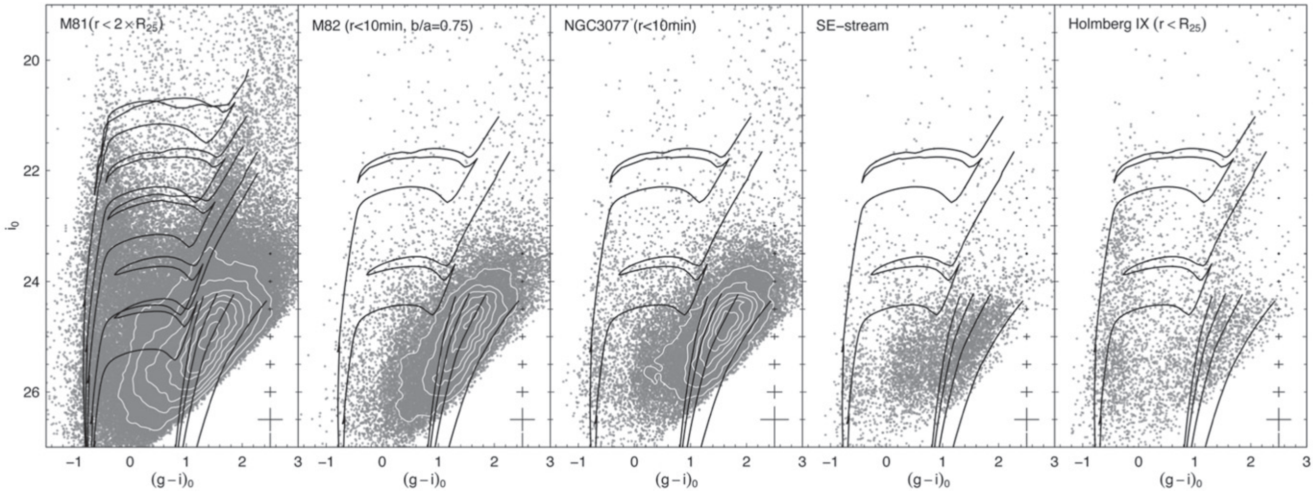

Figure 2. Dereddened CMDs of stellar sources in the disk and halo (see the text) of each galaxy and in the SE-stream. The overplotted isochrones are the same as those in Figure 1.

the RGB tip at $i_0 = 24.25$, intermediate-age ($\sim$0.5–8 Gyr) AGBs are found (Marigo et al. 2008). From the RGB tip to about 1.5 magnitude below, the blue and red RGB boxes contain stars older than 1 Gyr. We also examine the spatial distribution of BO sources. We note that the completeness of our photometry decreases toward the red, as shown by the dashed lines, so our RGB sample may be biased toward the bluer side.

Figure 2 shows the dereddened CMDs of the disk and halo of each galaxy, HoIX, and the stream between M81 and NGC 3077 (hereafter the SE-stream). Stars within $r = 2 \times R_{25}$ (i.e., $27'.6$ or 29 kpc) of M81, within $10'$ (10.5 kpc) of M82 and NGC 3077, and within $r = R_{25}$ ($2'.5$ or 2.6 kpc) of HoIX are shown (see dashed lines in Figure 3); an axis ratio of 0.75 has been used for M82 to take into account the varying flattening of the stellar distribution in the outer regions. We also select a $15' \times 6'$ area for the SE-stream between M81 and NGC 3077. Young, blue MS and RSG can be easily seen in the M81 CMD, as well as vast numbers of RGBs. In M82 and NGC 3077, RGBs are prominent and some MSs exist, but few, if any, RSGs can be seen. We note that the area within R_{25} of each galaxy could not be resolved due to crowding, so we miss the stars of the M81 and M82 disks and in the NGC 3077 center. In the SE-stream, the most luminous MSs correspond to $\sim$32 Myr old. In HoIX, several MSs, cHeBs, and RSGs exist. Although we cannot resolve RGBs at the innermost ($<1'$) HoIX, the number density of RGBs in HoIX are comparable to those of other regions at the same distance from M81. Therefore, as discussed by Sabbi et al. (2008) with deeper *HST* images, most of the old components at HoIX may belong to the M81 halo.

4. THE SPATIAL DISTRIBUTIONS OF YOUNG AND OLD COMPONENTS

Figure 3 shows the spatial distributions of HI gas (Yun et al. 1994), MS, cHeB, RSG, AGB, blue and red RGB stars, and BOs defined in Figure 1, without correction for the completeness and contaminants. In the upper panels, the solid ellipses represent the R_{25} radii of the three main galaxies.

The distribution of the young populations traced by the young MS, MS+cHeB, and RSG stars agrees extremely well with that of the HI distribution, except for the stream at the northwest of NGC 3077 where few stars are seen. The young MSs are mainly concentrated in the spiral arms of M81, at the northwest side (hereafter NW-arm), AL, HoIX, BK3N, the Garland, and SE-stream. A number of small clumps are also seen as they follow HI blobs around these systems. The stellar concentration in the NW-arm was identified by Davidge (2008b) and was suggested to be part of the M81 arm by Barker et al. (2009). We confirm that it is connected to the stellar concentration on the north arm. The higher-density regions in the SE-stream have been reported either as clumps or as a dwarf galaxy (d0959 + 68) in previous studies (Durrell et al. 2004; Mouhcine & Ibata 2009; Chiboucas et al. 2013). As Chiboucas et al. (2013) discussed, these overdensities are clearly parts of a single stream. Near NGC 3077, many MSs are found in the Garland and up to about 8 kpc to the south and 10 kpc to the east where HI gas and dust emission have been observed (Walter et al. 2011). In M82, a prominent stellar feature can be seen at $(\Delta\alpha, \Delta\delta) \sim (0.1, 0.6)$, identified as an arc by Sun et al. (2005) and Davidge (2008a). MSs are also distributed well beyond the R_{25} radius up to the projected distance of about 16 kpc from M82.

Stars in the MS+cHeB box have a very similar distribution to that of the young MSs. The arc at the southeast of M82 appears to have a clumpy shape, but it is an artificial appearance due to the overlap of plotted points (see Figure 5). Interestingly, our maps show that there is another young stellar feature on the opposite side of M82 that appears to be aligned with the southern arc and may therefore be related. The selection box of MS+cHeB stars includes some contamination, mainly from background blue objects, as can be seen by the low-level uniform distribution of sources through out the area. In the top right panel of Figure 3, the distribution of the RSGs is almost the same as that of MSs and cHeBs. However, the fainter substructures—SE-stream, M82-arc, some clumps around HoIX and AL, and BK3N—can not be seen in this map due to the shorter lifetime and the lower number of RSGs compared to MSs.

In contrast, the older populations (AGB, RGBs) have a much smoother distribution than the younger stars. Old stars are mainly embedded in the halos that reach far beyond the R_{25} radii of three galaxies. The sizes of these RGB halos are considerable, and they may even overlap (see Figure 4). While

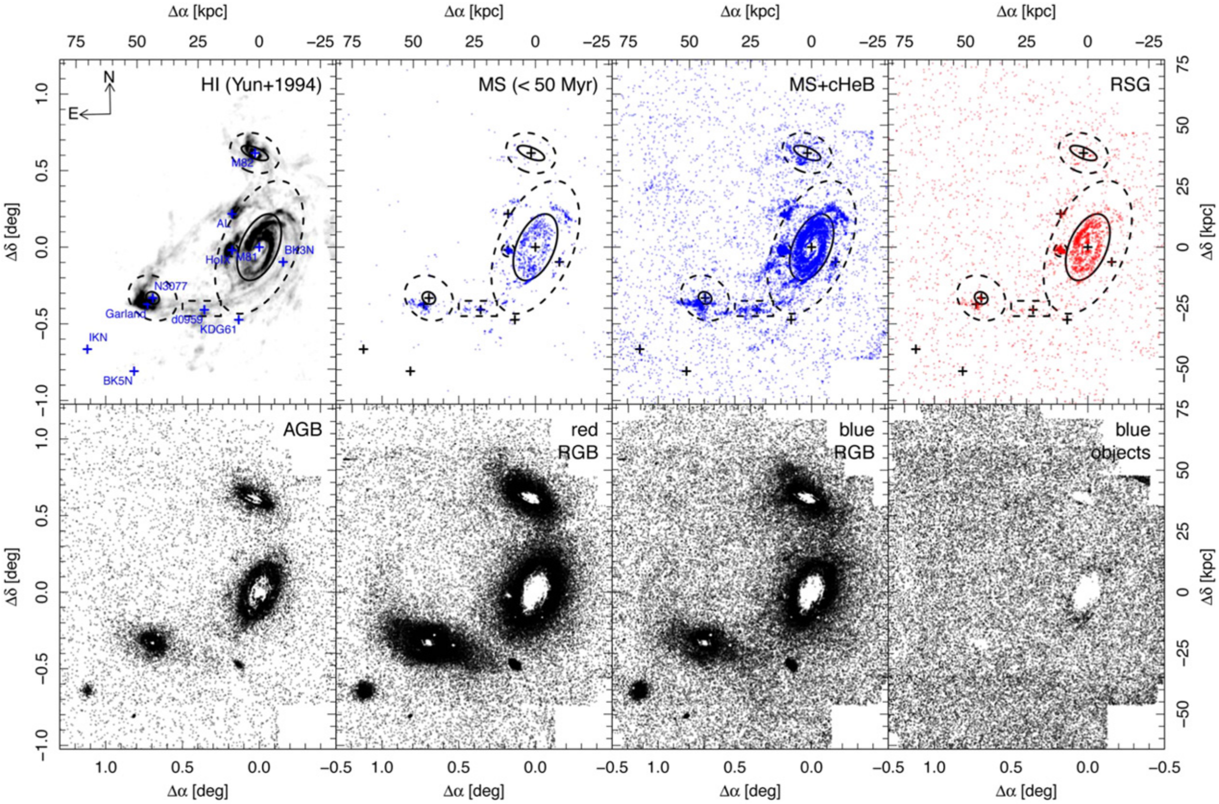

Figure 3. Spatial distribution of stars in each evolutionary phase selected in Figure 1. Shown from the top left to the bottom right are the HI column density map taken from Yun et al. (1994), the spatial distributions of stars in evolutionary phases, and blue contaminants. The cross marks represent the centers of known M81 group members. The solid lines are R_{25} of galaxies, with axis ratios of M82 and NGC 3077 of $b/a = 0.38$ and 0.83, and an inclination angle of $i = 58°$ for M81, respectively. The dashed lines outline the regions used for the CMDs in Figure 2.

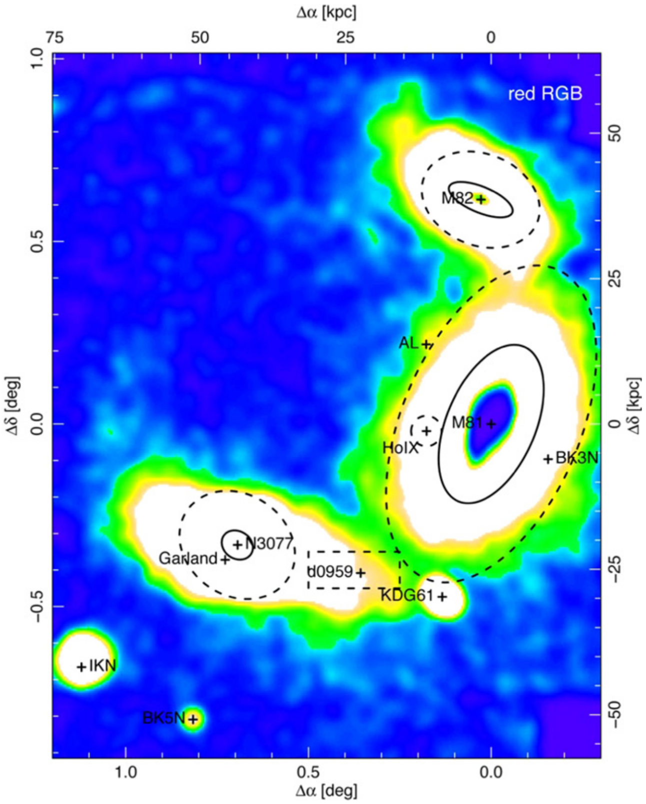

Figure 4. Isodensity contour map of red RGB stars, featured to faint structures up to 20σ above the background level. The kernel density is estimated with the bandwidth of $1'.2$. The marks and lines are the same as in Figure 3.

the M82 halo seems to be more extended in the blue RGB map, the halos of M81 and NGC 3077are more prominent in the red RGB map, suggesting they have a higher mean metallicity. In the contour map of red RGBs in Figure 4, a tidal stream between M81 and M82 can clearly be seen, and the outer regions of M82 and NGC 3077 exhibit an "S-shaped" morphology. The dwarf galaxies IKN, BK5N, and KDG 61 cannot be seen in the maps of young stars, but appear as overdensities of old populations, implying they have not formed as a result of the recent interaction.

In the bottom right panel of Figure 3, we plot the distribution of BOs at $25 < i_0 < 26$ and $0.2 < (g-i)_0 < 0.4$. The uniform distribution of these sources supports their identification as contaminants since the star/galaxy separation in our photometry degrades at a magnitude fainter than about 24 mag in both the g and i bands.

5. DISCUSSION AND SUMMARY

We find that the young intra-group population in the M81 group traces the filamentary structures of the HI gas connecting M81, M82, and NGC 3077, confirming the results of several smaller field-of-view studies. The left panel of Figure 5 shows the spatial distribution of stars in young MS and MS+cHeB boxes of Figure 1, which are color coded according to i-band magnitude in a transparent manner so that colors of overlapping points represent the average color. Bright stars are mainly located in the inner disk of M81, while most of young stars in AL, NW-arm, BK3N, Garland, and other debris features are fainter than $i_0 \sim 24$ and have similar luminosity distributions to

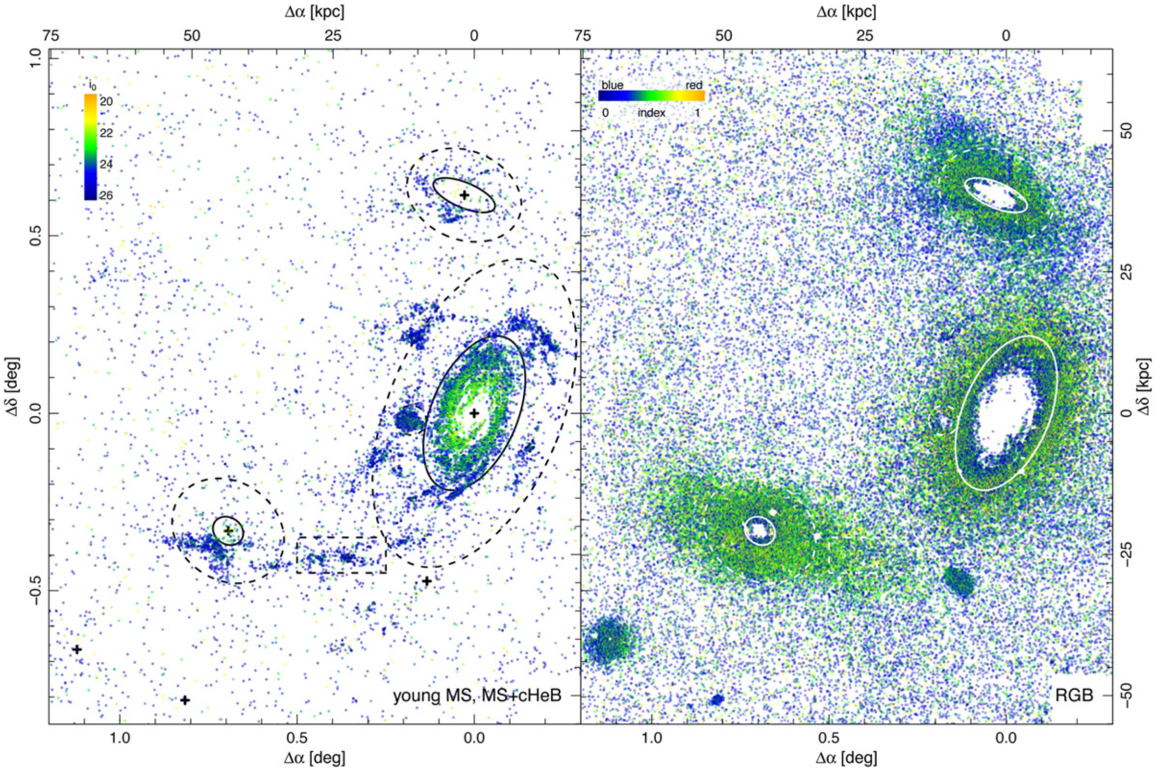

Figure 5. Left: the spatial distribution of MS and cHeB stars that are color coded according to the luminosity with transparency. Right: the spatial distribution of RGB stars. The color of each point represents the $(g-i)_0$ color of star with transparency. The marks and lines are the same as in Figure 3.

the SE-stream, implying ages of 30–160 Myr old. This suggests that star formation in these tidal features was synchronized and may have stopped about 30 Myr ago. The SE-stream is slightly inclined from the southeast to the northwest, whereas the tail of RGB stars in NGC 3077 at the same location is extended toward the northeast–southwest. That fact that these spatial distributions do not exactly match may indicate that the SE-stream comes from material torn from M81, while the RGB tail is material stripped from NGC 3077. The color of HoIX is slightly greener than other clumps and streams, meaning it includes some bright (younger) MS stars as we see in Figure 2.

The right panel of Figure 5 shows the color distribution of RGBs, which can be interpreted as a rough proxy for metallicity. The bluest (index = 0) and reddest (index = 1) colors correspond to [M/H] = −2.3 and −0.75, respectively, assuming 12 Gyr old age. The RGBs between the solid and dashed lines of M81, M82, and NGC 3077 have similar colors; the medians of the color indexes are 0.41, 0.40, and 0.46, respectively, corresponding to [M/H] ~ −1.4, −1.4, and −1.3. This M81 halo metallicity is slightly lower than the value of [M/H] ~ −1.1 derived from previous *Subaru* imagery and the estimation [Fe/H] = −1.2 from deep *HST* photometry (Barker et al. 2009; Monachesi et al. 2013). This might be due to the missing metal-rich RGB stars in our photometry since the completeness gets worse at redder colors. The halo of M82 has a color gradient from the inner greener area to the outer bluer region; the greener part is also extended toward the northeast and along the direction of the young stellar arc. Note that we do not correct for the internal extinction of each galaxy, so it is not possible from this study alone to determine if these are the bona fide features of the M82 halo. The tidal stream between M81 and M82 is also predominantly blue in color, indicating that this is material being stripped from M82 onto M81.

In Figures 4 and 5, the NGC 3077 halo is extended far beyond the R_{25} and has a rhombus shape stretched in the east–west direction. In the outermost region, an S-shape distortion can be discerned, which is similar to what was found around M33 (McConnachie et al. 2010). The component in the northwest appears to reach a maximum projected radius from NGC 3077 of ~65 kpc, but does not appear to trace the HI distribution in this region. The S-shaped structure is typical of an interacting dwarf galaxy with a larger companion (e.g., Peñarrubia et al. 2009). Numerical modeling suggests the encounters between NGC 3077, M81, and M82 took place ~200–300 Myr ago (Yun et al. 1999), which may not leave enough time to restore equilibrium in the NGC 3077 halo. We will return to the topic of the stellar streams in the M81 group in a later paper.

The close encounters between M81, M82, and NGC 3077 induced star formation in tidally stripped gas. As a consequence, new stellar concentrations were born out of these HI rich clumps, many of which lie far from the main bodies of the galaxies. Of these concentrations, only AL appears to have a clear counterpart in the RGB map. The presence of an older stellar component suggests that this object, like the dwarf galaxies IKN, BK5N, and KDG 61, may not have a tidal origin. The gravitational interactions between the M81 group galaxies have also significantly perturbed their older stellar components leading to disturbed halo morphologies and giant stellar streams that appear to connect all three systems. When combined with our forthcoming HSC observations of the west side of M81, these data will allow us to determine the true extent and nature of the intra-group debris and map the halos of the M81 group galaxies to unprecedented distances.

We are grateful to the entire staff at *Subaru* Telescope and the HSC team. We acknowledge the importance of Maunakea within the indigenous Hawaiian community. This paper makes use of software developed for the LSST. We thank the LSST Project for making their code available as free software at http://dm.lsstcorp.org. S.O. acknowledges support from the CAS PIFI scheme. A.M.N.F. and E.J.B. acknowledge support from an STFC Consolidated Grant. This work was supported by the grants of CAS (XDB09010100), NSFC (11333003), and JSPS (Grant-in-Aid for Young Scientists B, 26800103).

REFERENCES

Axelrod, T., Kantor, J., Lupton, R. H., & Pierfederici, F. 2010, Proc. SPIE, 7740, 15
Barker, M. K., Ferguson, A. M. N., Irwin, M., Arimoto, N., & Jablonka, P. 2009, AJ, 138, 1469
Barker, M. K., Ferguson, A. M. N., Irwin, M. J., Arimoto, N., & Jablonka, P. 2012, MNRAS, 419, 1489
Belokurov, V., Zucker, D. B., Evans, N. W., et al. 2007, ApJ, 654, 897
Bressan, A., Marigo, P., Girardi, L., et al. 2012, MNRAS, 427, 127
Bullock, J. S., & Johnston, K. V. 2005, ApJ, 635, 931
Chiboucas, K., Jacobs, B. A., Tully, R. B., & Karachentsev, I. D. 2013, AJ, 146, 126
Chynoweth, K. M., Langston, G. I., Yun, M. S., et al. 2008, AJ, 135, 1983
Crnojević, D., Ferguson, A. M. N., Irwin, M. J., et al. 2013, MNRAS, 432, 832
Davidge, T. J. 2008a, ApJL, 678, L85
Davidge, T. J. 2008b, PASP, 120, 1145
de Mello, D. F., Smith, L. J., Sabbi, E., et al. 2008, AJ, 135, 548
de Vaucouleurs, G., de Vaucouleurs, A., Corwin, H. G., Jr., et al. 1991, Third Reference Catalogue of Bright Galaxies (New York: Springer)
Durrell, P. R., Decesar, M. E., Ciardullo, R., Hurley-Keller, D., & Feldmeier, J. J. 2004, IAU Symp. 217, Recycling Intergalactic and Interstellar Matter, ed. P.-A. Duc, J. Braine, & E. Brinks (San Francisco, CA: ASP), 90
Durrell, P. R., Sarajedini, A., & Chandar, R. 2010, ApJ, 718, 1118
Ferguson, A. M. N., Irwin, M. J., Ibata, R. A., Lewis, G. F., & Tanvir, N. R. 2002, AJ, 124, 1452
Fitzpatrick, E. L. 1999, PASP, 111, 63
Freedman, W. L., Hughes, S. M., Madore, B. F., et al. 1994, ApJ, 427, 628
Ibata, R., Irwin, M., Lewis, G., Ferguson, A. M. N., & Tanvir, N. 2001, Natur, 412, 49
Ibata, R. A., Lewis, G. F., McConnachie, A. W., et al. 2014, ApJ, 780, 128
Ivezic, Z., Tyson, J. A., Abel, B., et al. 2008, arXiv:0805.2366
Karachentsev, I. D., Karachentseva, V. E., & Boerngen, F. 1985, MNRAS, 217, 731
Karachentsev, I. D., Karachentseva, V. E., Huchtmeier, W. K., & Makarov, D. I. 2004, AJ, 127, 2031
Kudritzki, R.-P., Urbaneja, M. A., Gazak, Z., et al. 2012, ApJ, 747, 15
Makarova, L. N., Grebel, E. K., Karachentsev, I. D., et al. 2002, A&A, 396, 473
Marigo, P., Girardi, L., Bressan, A., et al. 2008, A&A, 482, 883
Martínez-Delgado, D., Gabany, R. J., Crawford, K., et al. 2010, AJ, 140, 962
McConnachie, A. W., Ferguson, A. M. N., Irwin, M. J., et al. 2010, ApJ, 723, 1038
McConnachie, A. W., Irwin, M. J., Ibata, R. A., et al. 2009, Natur, 461, 66
Mihos, J. C., Harding, P., Feldmeier, J., & Morrison, H. 2005, ApJL, 631, L41
Miyazaki, S., Komiyama, Y., Nakaya, H., et al. 2012, Proc. SPIE, 8446, 844602
Monachesi, A., Bell, E. F., Radburn-Smith, D. J., et al. 2013, ApJ, 766, 106
Mouhcine, M., & Ibata, R. 2009, MNRAS, 399, 737
Mouhcine, M., Ibata, R., & Rejkuba, M. 2010, ApJL, 714, L12
Okamoto, S., Arimoto, N., Yamada, Y., & Onodera, M. 2012, ApJ, 744, 96
Peñarrubia, J., Navarro, J. F., McConnachie, A. W., & Martin, N. F. 2009, ApJ, 698, 222
Pillepich, A., Vogelsberger, M., Deason, A., et al. 2014, MNRAS, 444, 237
Radburn-Smith, D. J., de Jong, R. S., Seth, A. C., et al. 2011, ApJS, 195, 18
Sabbi, E., Gallagher, J. S., Smith, L. J., de Mello, D. F., & Mountain, M. 2008, ApJL, 676, L113
Sakai, S., & Madore, B. F. 2001, ApJ, 555, 280
Schlafly, E. F., & Finkbeiner, D. P. 2011, ApJ, 737, 103
Stetson, P. B. 1987, PASP, 99, 191
Sun, W.-H., Zhou, X., Chen, W.-P., et al. 2005, ApJL, 630, L133
van der Hulst, J. M. 1979, A&A, 75, 97
Walter, F., Sandstrom, K., Aniano, G., et al. 2011, ApJL, 726, L11
Weisz, D. R., Skillman, E. D., Cannon, J. M., et al. 2008, ApJ, 689, 160
Williams, B. F., Dalcanton, J. J., Seth, A. C., et al. 2009, AJ, 137, 419
York, D. G., Adelman, J., Anderson, J. E., Jr., et al. 2000, AJ, 120, 1579
Yun, M. S. 1999, IAU Symp. 186, Galaxy Interactions at Low and High Redshift, ed. J. E. Barnes & D. B. Sanders (Dordrecht: Kluwer), 81
Yun, M. S., Ho, P. T. P., & Lo, K. Y. 1994, Natur, 372, 530